The Astrophysical Journal, 938:12 (6pp), 2022 October 10 https://doi.org/10.3847/1538-4357/ac9133

GW170817 4.5 Yr After Merger: Dynamical Ejecta Afterglow Constraints

Arvind Balasubramanian[1], Alessandra Corsi[1], Kunal P. Mooley[2], Kenta Hotokezaka[3], David L. Kaplan[4], Dale A. Frail[5], Gregg Hallinan[2], Davide Lazzati[6], and Eric J. Murphy[7]
[1] Department of Physics and Astronomy, Texas Tech University, Box 1051, Lubbock, TX, 79409-1051, USA; arvind.balasubramanian@ttu.edu
[2] Caltech, 1200 E. California Blvd. MC 249-17, Pasadena, CA, 91125, USA
[3] Research Center for the Early Universe, Graduate School of Science, University of Tokyo, Bunkyo-ku, Tokyo 113-0033, Japan
[4] Center for Gravitation, Cosmology, and Astrophysics, Dept. of Physics, University of Wisconsin-Milwaukee, P.O. Box 413, Milwaukee, WI, 53201, USA
[5] National Radio Astronomy Observatory, Socorro, NM, 87801, USA
[6] Department of Physics, Oregon State University, 301 Weniger Hall, Corvallis, OR, 97331, USA
[7] National Radio Astronomy Observatory, Charlottesville, VA, 22903, USA
Received 2022 May 29; revised 2022 September 9; accepted 2022 September 10; published 2022 October 11

Abstract

GW170817 is the first binary neutron star (NS) merger detected in gravitational waves (GWs) and photons, and so far remains the only GW event of its class with a definitive electromagnetic counterpart. Radio emission from the structured jet associated with GW170817 has faded below the sensitivity achievable via deep radio observations with the most sensitive radio arrays currently in operation. Hence, we now have the opportunity to probe the radio re-brightening that some models predict, which should emerge at late times from the interaction of the dynamically stripped merger ejecta with the interstellar medium. Here we present the latest results from our deep radio observations of the GW170817 field with the Karl G. Jansky Very Large Array (VLA), 4.5 yr after the merger. Our new data at 3 GHz do not show any compelling evidence for emission in excess to the tail of the jet afterglow (<3.3 μJy), confirming our previous results. We thus set new constraints on the dynamical ejecta afterglow models. These constraints favor single-speed ejecta with energies $\lesssim 10^{50}$ erg (for an ejecta speed of $\beta_0 = 0.5$), or steeper energy–speed distributions of the kilonova ejecta. Our results also suggest larger values of the cold, nonrotating maximum NS mass in equal-mass scenarios. However, without a detection of the dynamical ejecta afterglow, obtaining precise constraints on the NS equation of state remains challenging.

Unified Astronomy Thesaurus concepts: Radio continuum emission (1340); Radio transient sources (2008); X-ray transient sources (1852)

1. Introduction

GW170817 remains the first and only example of the merger of two neutron stars (NSs), observed by LIGO and VIRGO (Abbott et al. 2017b), whose discovery in gravitational waves (GWs) was followed by the identification of a definitive electromagnetic (EM) counterpart from radio to γ-ray frequencies.

The treasure trove of information that this event has provided to the astronomy community cannot be understated. We refer the reader to the many papers written on this event for a comprehensive description of all of the observations that enabled the identification of a coincident gamma-ray burst (GRB; e.g., Abbott et al. 2017a, and references therein); a host galaxy at 40 Mpc and a UV/optical/IR kilonova (e.g., Arcavi et al. 2017; Chornock et al. 2017; Coulter et al. 2017; Cowperthwaite et al. 2017; Drout et al. 2017; Kasliwal et al. 2017; Kasen et al. 2017; Kilpatrick et al. 2017; Metzger 2017; Pian et al. 2017; Shappee et al. 2017; Smartt et al. 2017; Tanvir et al. 2017; Valenti et al. 2017); and a delayed nonthermal afterglow observed from radio to X-rays (e.g., Margutti et al. 2017; Haggard et al. 2017; Troja et al. 2017; Hallinan et al. 2017).

Extensive observations of the quasi-thermal kilonova and of the nonthermal afterglow associated with GW170817 have painted a detailed picture of the ejecta that resulted from the merger of the two NSs in the compact binary progenitor of GW170817. While the kilonova was powered by quasi-isotropic and relatively slow neutron-rich debris originating from a combination of dynamical ejecta and disk winds (e.g., Metzger 2017), the nonthermal radio afterglow probed the existence of an off-axis jet that successfully burrowed through the neutron-rich debris. Radio observations, in particular, were instrumental in narrowing down the morphology of relativistic ejecta to a structured jet (a.k.a. jet+cocoon), and in providing crucial insights into the geometry of the merger itself, and the density of the interstellar medium (ISM) through which the jet was launched (Alexander et al. 2017; Corsi et al. 2018; Dobie et al. 2018; Lazzati et al. 2018; Margutti et al. 2018; Mooley et al. 2018a, 2018b, 2018c; Ghirlanda et al. 2019; Hajela et al. 2019; Ren et al. 2020).

Well before the discovery of GW170817, models had been proposed predicting that, regardless of whether a jet is successfully launched in a binary NS merger, the interaction of the kilonova ejecta with the ISM can produce nonthermal emission in the radio a few years after merger (e.g., Nakar & Piran 2011; Piran et al. 2013; Hotokezaka & Piran 2015), motivating several related observational efforts in cosmological short GRBs (e.g., Metzger & Bower 2014; Fong et al. 2016; Horesh et al. 2016). With GW170817, these late-time re-brightening models have spurred new interest in the community (Hotokezaka et al. 2018; Bartos et al. 2019; Kathirgamaraju et al. 2019; Liu et al. 2020; Margalit & Piran 2020), especially given their potential to probe the nature of the merger remnant in relation to the equation of state (EoS) of nuclear matter (see, e.g., Nedora et al. 2021, and references therein). Thus, additional observational campaigns have been carried out in search for late-time radio afterglows for both GW170817 (Balasubramanian et al. 2021; Hajela et al. 2022; Troja et al.

Table 1
VLA Late-time Observations of the GW170817 Field

Date (UT)	ν (GHz)	VLA config.	Time on Source (hr)	rms (μJy)	VLA program	PI	Nominal synth. beam ($''$)
2021 Dec 6	3.0	B	$2^h24^m54^s$	4.9 (3.6)	21B-057	Balasubramanian	2.1
2021 Dec 20	3.0	B	$2^h25^m57^s$	4.4 (3.9)	21B-057	Balasubramanian	2.1
2021 Dec 28	3.0	B	$2^h25^m57^s$	4.7 (3.9)	21B-057	Balasubramanian	2.1
2022 Jan 5	3.0	B	$2^h25^m57^s$	4.9 (4.3)	21B-057	Balasubramanian	2.1
2022 Mar 5	2.9	A	$2^h28^m00^s$	4.4 (3.9)	22A-168	Balasubramanian	0.65
2022 Mar 10	3.0	A	$2^h28^m08^s$	4.4 (3.9)	22A-168	Balasubramanian	0.65
2022 Mar 14	3.0	A	$2^h28^m02^s$	4.0 (3.9)	22A-168	Balasubramanian	0.65
2022 Mar 17	3.0	A	$2^h28^m08^s$	4.0 (3.9)	22A-168	Balasubramanian	0.65
2022 Mar 22	3.0	A	$2^h28^m10^s$	4.1 (4.0)	22A-168	Balasubramanian	0.65
2022 Mar 23	3.0	A	$2^h17^m34^s$	4.4 (4.1)	22A-168	Balasubramanian	0.65
2022 Mar 28	3.0	A	$2^h38^m42^s$	3.7 (3.4)	22A-168	Balasubramanian	0.65
2022 Mar 29	3.0	A	$2^h28^m00^s$	3.9 (3.7)	22A-168	Balasubramanian	0.65

Note. See the text for details regarding the rms measurements.

2022) and other short GRBs (e.g., Klose et al. 2019; Bruni et al. 2021; Grandorf et al. 2021; Ricci et al. 2021), albeit without any definitive detections so far.

Motivated by the above considerations, in Balasubramanian et al. (2021) we presented the deepest radio observations of the GW170817 field at 3.5 yr after merger, and found no evidence for a late-time radio re-brightening. This result helped constrain the energy–speed distribution of the kilonova ejecta (Balasubramanian et al. 2021), and provided hints on the NS EoS (Nedora et al. 2021). On the other hand, late-time X-ray observations of the GW170817 field around the same epoch had left open the possibility of late-time emission in excess to that expected from the tail of the GW170817 jet afterglow (Hajela et al. 2022; Troja et al. 2022). However, continued follow-up in the X-rays at 4.3–4.8 yr since the merger did not confirm the presence of any X-ray excess at these later times (Hajela et al. 2021; O'Connor & Troja 2022).

Here, we present new deep observations of the GW170817 field carried carried out with the Karl G. Jansky Very large Array (VLA) at 3 GHz and at the epoch of about 4.5 yr since the merger. These observations improve substantially on the sensitivity reached by recently reported radio observations of the same field (Ricci et al. 2022). Our paper is organized as follows. We report our new observations in Section 2; in Section 3 we discuss our results within the kilonova ejecta afterglow model; finally, in Section 4 we summarize and conclude.

2. Observations and Data Reduction

We carried out radio continuum observations of the GW170817 field with the VLA. Our observations were executed with the standard VLA S-band setup, with a nominal central frequency of 3 GHz, and split in 12 epochs (each providing approximately 2.5 hr on source) between 2021 December and 2022 March. The first four epochs were observed with the VLA in its B configuration, while the subsequent eight epochs were carried out with the array in its most extended A configuration. These observations are listed in Table 1. After calibration was performed with the automated VLA calibration pipeline, we manually inspected the data and performed further flagging for radio frequency interference (RFI) as needed. We then imaged the data using the `CASA` (McMullin et al. 2007) task `tclean` with one Taylor term (`nterms = 1`) and robust weighting (`robust = 0.5`; see also Balasubramanian et al. 2021), and

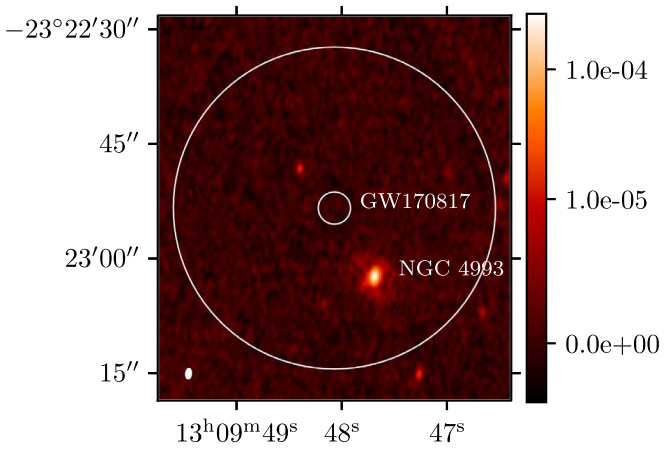

Figure 1. Image of the GW170817 field at ≈4.5 yr since the merger, as derived from our deepest co-added data set (see Table 2). The small circle has a radius of 2.″1 and is centered on the position of GW170817. The larger circle has a radius of 21″, equal to the radius of the circular region used to calculate our rms sensitivity in the residual image of the field. The host galaxy of GW170817 is enclosed in this larger circular region. Several sources unrelated to GW170817 are also visible. The synthesized beam ellipse is shown in the bottom left. The color bar gives the flux density in Jy.

derived the sensitivity rms measurements running `imstat` on the residual images within a circular region of radius equal to 10 nominal synthesized beams[8] around the position of GW170817 ($\alpha = 13^h09^m48^s.069$, $\delta = -23^d22^m53^s.39$ J2000; Mooley et al. 2018c). Because this region may include residuals associated with the host galaxy light (see Figure 1), we also list in parenthesis in Table 1 the rms values we obtain using a circular region of the same size in a source-free portion of the image. We find no significant ($>3\times$ rms) excess in a region of one synthesized beam around the position of GW170817 in any of the individual epochs.

Next, we co-add the four B configuration observations, and the eight A configuration observations separately; finally, we co-add the full multiple configuration data set (all in the visibility domain) for a total of 12 observations. The imaging for these co-added data sets was performed similar to what is described above, with the `CASA` task `tclean` but using `nterms = 2` to clean the emission from bright radio sources in the field better. To estimate the rms sensitivity for the co-added

[8] As recommended by Hancock et al. (2012) and Mooley et al. (2013).

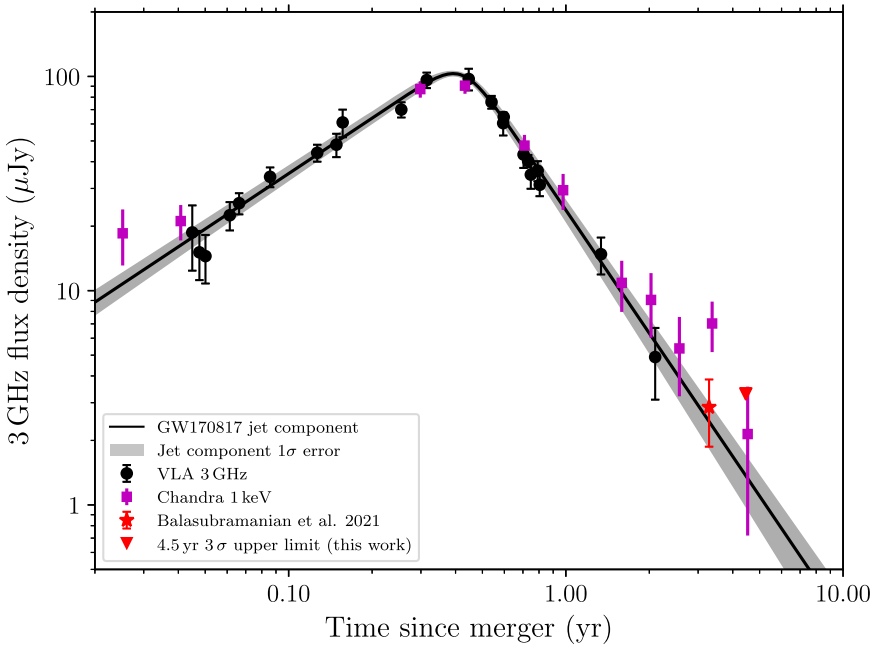

Figure 2. 3 GHz radio light curve of GW170817 with the best-fit structured jet model from Makhathini et al. 2021. The radio data are shown as black data points. The Chandra 1 keV data scaled to 3 GHz with a power-law index of $\beta = -0.584$ (including the latest measurement by O'Connor & Troja 2022) are shown as purple squares (see, e.g., Haggard et al. 2017; Margutti et al. 2017; Troja et al. 2017, 2022; Hajela et al. 2022, and references therein). We extrapolate all X-ray data to 3 GHz using $\beta = -0.584$ because there is only marginal evidence for a potential spectral flattening around 3.5 yr since the merger (Balasubramanian et al. 2021; Hajela et al. 2022) which, however, has not been confirmed in later observations by O'Connor & Troja (2022). Our previous observation 3.5 yr since the merger is marked with a red star (Balasubramanian et al. 2021). The 3σ upper limit from this work is shown as red a downward pointing triangle.

Table 2
Results for the Co-added Late-time Radio Observations of GW170817

Date (UT)	Epoch (yr)	ν (Hz)	F_ν (μJy)	σ_ν (μJy)	Instrument	Reference
2021 Dec 6–2022 Jan 5	4.3	2.8×10^9	<6.6	2.2	VLA B	This work
2022 Mar 5–2022 Mar 29	4.6	3.0×10^9	<4.5	1.5	VLA A	This work
2021 Dec 6–2022 Mar 29	4.5	3.0×10^9	<3.3	1.1	VLA A&B	This work
2021 Dec 7–2022 May 18	4.5	2.41×10^{17}	5.18×10^{-5}	3.44×10^{-5}	Chandra	O'Connor & Troja (2022)

Note. See the text for discussion.

observations in the A and B configurations, we conservatively use a circular region of radius 10 times the nominal synthesized beamwidth of the B configuration, centered on the location of GW170817 in the residual images (Figure 1 and Table 2). We note that the rms values estimated this way differ by less than 10% from the rms values calculated in source-free regions of the cleaned image. In our deepest co-added image we reach an rms sensitivity of 1.1 μJy at 3.0 GHz. No emission in excess to 3$\times$ the co-added image rms is found in a circular region of radius 2.″1 (FWHM of the nominal VLA synthesized beam in the B configuration at 3 GHz) around the location of GW170817. Specifically, at the location of GW170817 we measure a 3 GHz flux of 2.1 ± 1.1 μJy. Therefore, we constrain the radio emission from GW170817 to <3.3 μJy at 4.5 yr since the merger (see Figure 2).

3. Discussion

In Figure 2, we show the 3 GHz light curve of GW170817 (see the panchromatic afterglow data webpage[9] for a compilation of the full data set). The black data points are the previous radio observations (Hallinan et al. 2017; Mooley et al. 2018a, 2018b; Makhathini et al. 2021) that follow the jet +cocoon afterglow model (black line with gray 1σ error region). The red star shows our previous radio detection at ~3.5 yr since the merger (Balasubramanian et al. 2021). The radio upper limit from this work is shown with a downward pointing red triangle. As evident from this figure, we do not find any significant evidence for emission in excess of the expectations from a decaying jet+cocoon afterglow model, confirming our previous results (Balasubramanian et al. 2021).

For comparison, in Figure 2 we also show the X-ray flux measurements derived from Chandra observations of the GW170817 field, shown as purple squares (see, e.g., Haggard et al. 2017; Margutti et al. 2017; Troja et al. 2017, 2022; Hajela et al. 2022, and references therein), extrapolated to the radio band using a radio-to-X-ray spectral index of $\beta = -0.584$ (see Makhathini et al. 2021). Recently, O'Connor & Troja 2022 also reported a measurement of $\sim 0.6 \times 10^{15}$ erg cm^{-2}s^{-1} for the 0.3–10 keV flux of GW170817 at ≈4.8 yr after the merger (assuming a spectral index of −0.585), using observations carried out with the Chandra observatory (Hajela et al. 2021;

[9] http://www.tauceti.caltech.edu/kunal/gw170817/gw170817_afterglow_data_full.txt and https://github.com/kmooley/GW170817/.

O'Connor & Troja 2022). We convert this flux into a flux density at 1 keV (see Table 2), and, by combining it with the radio upper limit presented here, we derive a radio-to-X-ray spectral index of $\beta \gtrsim -0.608$. This is compatible with the best-fit value obtained via previous observations of the structured jet afterglow ($\beta = -0.584 \pm 0.002$; Makhathini et al. 2021), and with the results of our analysis at 3.5 yr after the merger ($\beta = -0.535 \pm 0.024$; Balasubramanian et al. 2021).

Hereafter we discuss the implications of our latest radio observations in the context of the kilonova ejecta model, following the formulation of Kathirgamaraju et al. (2019). In this model, the kilonova blast wave drives a shock through the ISM, resulting in synchrotron emission. Electrons are accelerated to a power-law distribution of Lorentz gamma factors $\gamma_e > \gamma_{e,m}$, with power-law index p. The energy in the kilonova spherical blast wave is distributed as $E(>\beta\gamma) \propto (\beta\gamma)^{-\alpha}$ (with γ being the Lorentz factor, β being the speed in units of speed of light of the shocked fluid, and α being the power-law index of the energy–speed distribution) and normalized to the total energy E at some minimum velocity β_0 such that $E(>\beta_0\gamma_0) = E$. It is reasonable to assume that radio (GHz) observations are in between the minimum frequency, ν_m (corresponding to γ_m; see Nakar & Piran 2011), and the cooling frequency, ν_c. In this case, the kilonova peak flux density reads (Nakar & Piran 2011):

$$F_{\nu,pk} \approx (1.5\ \mathrm{mJy})\, \epsilon_{\mathrm{e},-1}^{p-1}\, \epsilon_{\mathrm{B},-3}^{\frac{p+1}{4}}\, n_{-2}^{\frac{p+1}{4}}\, \beta_0^{\frac{5p-7}{2}}\, E_{51}\, \nu_{9.5}^{\frac{1-p}{2}}\, d_{26}^{-2}, \quad (1)$$

where $Q_x = Q/10^x$ is followed for all quantities (Q, all expressed in cgs units), ϵ_B and ϵ_e are the fractions of the total energy in the magnetic field and electrons respectively, n is the number density of the medium, d is the distance to the source, and the normalization constant is calculated for $p = 2.1$. The time at which the kilonova afterglow emission peaks can be calculated as (Kathirgamaraju et al. 2019):

$$t_{\mathrm{dec}} = t_{\mathrm{pk}} \approx (3.3\mathrm{yr}) \left(\frac{E_{51}}{n_{-2}}\right)^{\frac{1}{3}} \beta_0^{-\frac{2}{3}} \left(\frac{2+\alpha}{\beta_0(5+\alpha)} - 1\right), \quad (2)$$

where α is the power-law index of the energy–speed distribution discussed earlier. The blast wave can be approximated to be mildly relativistic before this peak, and therefore the rising part of the kilonova ejecta light curve can be easily modeled as (see Kathirgamaraju et al. 2019 and references therein):

$$F_{\nu,\mathrm{KN}}(t) = F_{\nu,\mathrm{pk}} \left(\frac{t}{t_{\mathrm{p}}}\right)^s, \quad (3)$$

where:

$$s = \frac{3\alpha - 6(p-1)}{8+\alpha}. \quad (4)$$

For $\alpha = \infty$, Equations (1)–(3) reduce to the case of a spherical outflow of total energy E with uniform velocity β_0 (Nakar & Piran 2011). In this case, our flux upper limit at 4.5 yr constrains the energy E and speed β_0 for a given choice of the density and microphysical parameters. Indeed, setting these parameters as in Makhathini et al. (2021), an energy of $E \approx 10^{50}$ erg and speed of $\beta_0 \approx 0.5$ would produce a radio peak flux comparable to our 3σ upper limit at 4.5 yr since the merger. Hence, single-speed ejecta more energetic than $E \approx 10^{50}$ erg must be slower than $\beta_0 \approx 0.5$. Else, the radio emission from such ejecta would have peaked before 4.5 yr in the radio, at a flux level above 3.3 μJy.

Next, in Figure 3 we consider the case of a stratified ejecta with an energy–speed distribution described by the parameter $\alpha < \infty$. In this case, we can use our observations to constrain the values of α under specific assumptions on the energy and minimum speed of the ejecta, and of the density and microphysical parameters. The blue and green curves in the left panel of Figure 3 show the rising portion of the predicted kilonova afterglow. Specifically, the shades of solid blue curves assume the parameters $E = 10^{51}$ erg, $\beta_0 = 0.3$, $p = 2.1$, $\epsilon_e = 7.8 \times 10^{-3}$, $\epsilon_B = 9.9 \times 10^{-4}$, $n = 9.8 \times 10^{-3}\,\mathrm{cm}^{-3}$, and $d = 40$ Mpc (as in Makhathini et al. 2021); the dotted green and red curves assume the parameters $E = 10^{51}$ erg, $\beta_0 = 0.3$, $p = 2.2$, $\epsilon_e = 10^{-1}$, $\epsilon_B = 10^{-3}$, $n = 10^{-2}\mathrm{cm}^{-3}$, and $d = 40$ Mpc (as in Kathirgamaraju et al. 2019). The radio observations presented here (red downward pointing triangle for our 3σ upper limit) constrain α to $\alpha \gtrsim 6$ if we assume the parameters as in Makhathini et al. (2021). This is compatible with the constraints one can derive from the X-ray observations reported by O'Connor & Troja (2022) within the large error bars that affect this X-ray measurement (see the last purple square in Figure 3). For the more general choice of the microphysical parameters (Kathirgamaraju et al. 2019), our latest upper limit is compatible only with the more extreme cases of very steep values of α or with a kilonova blast wave comprised of a single velocity component ($\alpha = \infty$).

The results presented here can also improve on the constraints discussed by Nedora et al. 2021 regarding the NS EoS. In the right panel of Figure 3 we show a plot of the EoS-dependent model radio light curves from Nedora et al. (2021), compared with the radio upper limit derived in this analysis. As evident from this figure, our radio observations at 4.5 yr since the merger add new constraints on the possible EoSs, disfavoring the softer EoS SFHo (with $p = 2.05$, $\epsilon_e = 0.1$, $\epsilon_B = 0.01-0.001$, and $n = (4\text{–}5) \times 10^{-3}$ cm^{-3}), as well as the stiffer LS220 (with $p = 2.05$, $\epsilon_e = 0.1$, $\epsilon_B = 0.01-0.001$, and $n = 5 \times 10^{-3}$ cm^{-3}) in moderate mass-ratio scenarios ($q \lesssim 1.43$). The SFHo and LS220 EoSs predict the same maximum mass of the cold nonrotating NS, but LS220 correlates with a steeper ejecta energy–speed distribution for $q = 1$ (Radice et al. 2018). On the other hand, scenarios like a DD2 EoS with $q = 1$, that predict a larger value of the cold, nonrotating maximum NS mass, are still possible.

4. Summary and Conclusion

In this work, we have presented deep, 3 GHz observations of GW170817 at ≈4.5 yr since the merger. We co-added all the data collected with the VLA via our programs to obtain a deep image of the field, and find no evidence for a re-brightening that can be associated with the kilonova ejecta afterglow in the radio. This confirms our previous results (Balasubramanian et al. 2021). Overall, the upper limit we set here and the latest X-ray observations reported by O'Connor & Troja (2022) reinforce the conclusion that there is no clear evidence for a late-time re-brightening of the GW170817 nonthermal afterglow emission. Qualitatively speaking, models that envision the emergence of a new emission component at late times, with constant or declining X-ray emission beyond the epoch of ≈3.5 yr since the merger and without accompanying bright radio emission, could likely still be fit to the data (Hajela et al.

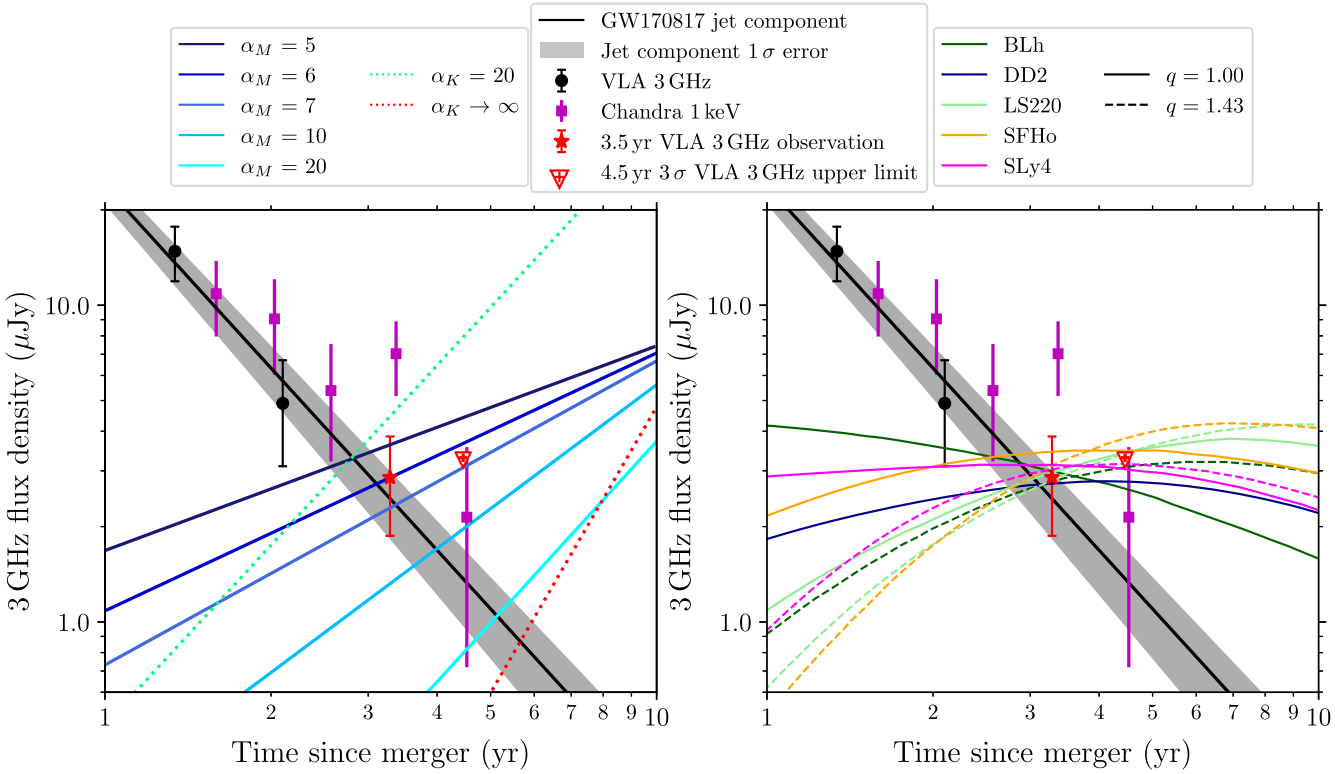

Figure 3. Late-time observations of the GW170817 field at 3 GHz from Makhathini et al. (2021) (black dots), Balasubramanian et al. (2021) (red star), and from this work (red downward pointing triangle for our 3σ upper limit). Chandra 1 keV observations scaled to 3 GHz with a power-law index of $\beta = -0.584$ (including the latest measurement by O'Connor & Troja 2022) are shown as purple squares (see, e.g., Haggard et al. 2017; Margutti et al. 2017; Troja et al. 2017, 2022; Hajela et al. 2022, and references therein). We extrapolate all X-ray data to 3 GHz using $\beta = -0.584$ because there is only marginal evidence for a potential spectral flattening around 3.5 yr since the merger (Balasubramanian et al. 2021; Hajela et al. 2022), which, however, has not been confirmed in the later observations by O'Connor & Troja (2022). We compare these observations with predicted kilonova afterglow light curves. Left: the solid lines in various shades of blue are the predicted kilonova afterglow light curves as a function of α (see Equation (3)) with the assumption that the minimum speed of the ejecta is $\beta_0 = 0.3$, for the parameters $E = 10^{51}$ erg, $p = 2.1$, $\epsilon_e = 7.8 \times 10^{-3}$, $\epsilon_B = 9.9 \times 10^{-4}$, $n = 9.8 \times 10^{-3}\mathrm{cm}^{-3}$, and $d = 40$ Mpc (as in Makhathini et al. 2021) and $\alpha_M = 5$, 6, 7, 10, and 20 (the subscript M indicates the parameters from Makhathini et al. 2021). For comparison, the green and red dashed lines show the case of $E = 10^{51}$ erg, $\epsilon_e = 10^{-1}$, $\epsilon_B = 10^{-3}$, $n = 10^{-2}\mathrm{cm}^{-3}$, $p = 2.2$, and $d = 40$ Mpc (as in Kathirgamaraju et al. 2019), with $\alpha_K = 20$, ∞ (the subscript K indicates the parameters from Kathirgamaraju et al. 2019; see Section 3); Right: predicted radio light curves of binary NS ejecta for different EoS and mass ratios reproduced from Nedora et al. (2021) (see their Figure 4 and Table 2). See Section 3 for discussion.

2022), but would be very hard to test via further radio (or X-ray) observations of the GW170817 field.

Kilonova ejecta afterglow models could still be constrained with further radio observations of sensitivity similar to the one reached in this work (and thus not without a substantial investment of observing time). Indeed, the observations presented here tighten the constraints on the power-law index of the energy–speed distribution of the kilonova ejecta to $\alpha \gtrsim 6$, somewhat steeper than the $\alpha \gtrsim 5$ constraint that we obtained at 3.5 yr post-merger (see Balasubramanian et al. 2021), and favor an EoS predicting larger values of the cold, nonrotating NS mass for $q = 1$ scenarios.

In the future, a radio non-detection at 7.5 yr since the merger would constrain the ejecta energy–speed distribution to $\alpha \gtrsim 10$ for reasonable assumptions on the ejecta parameters. A detection would also facilitate more precise constraints on the possible EoSs (see, e.g., BLh in the right panel of Figure 3), though previous considerations regarding the challenges of pinpointing a specific EoS remain true (see, e.g., Balasubramanian et al. 2021; Nedora et al. 2021).

A.B. and A.C. acknowledge support from NSF AST-1907975. K.P.M. and G.H. acknowledge support from the National Science Foundation grant AST-1911199. D.L. acknowledges support from NSF grant AST-1907955. D.K. is supported by NSF grant AST-1816492. The National Radio Astronomy Observatory is a facility of the National Science Foundation operated under cooperative agreement by Associated Universities, Inc.

ORCID iDs

Arvind Balasubramanian https://orcid.org/0000-0003-0477-7645
Alessandra Corsi https://orcid.org/0000-0001-8104-3536
Kunal P. Mooley https://orcid.org/0000-0002-2557-5180
Kenta Hotokezaka https://orcid.org/0000-0002-2502-3730
David L. Kaplan https://orcid.org/0000-0001-6295-2881
Gregg Hallinan https://orcid.org/0000-0002-7083-4049
Davide Lazzati https://orcid.org/0000-0002-9190-662X
Eric J. Murphy https://orcid.org/0000-0001-7089-7325

References

Abbott, B. P., Abbott, R., Abbott, T. D., et al. 2017a, ApJL, 848, L13
Abbott, B. P., Abbott, R., Abbott, T. D., et al. 2017b, PhRvL, 119, 161101
Alexander, K. D., Berger, E., Fong, W., et al. 2017, ApJL, 848, L21
Arcavi, I., Hosseinzadeh, G., Howell, D. A., et al. 2017, Natur, 551, 64
Balasubramanian, A., Corsi, A., Mooley, K. P., et al. 2021, ApJL, 914, L20
Bartos, I., Lee, K. H., Corsi, A., Márka, Z., & Márka, S. 2019, MNRAS, 485, 4150
Bruni, G., O'Connor, B., Matsumoto, T., et al. 2021, MNRAS, 505, L41
Chornock, R., Berger, E., Kasen, D., et al. 2017, ApJL, 848, L19
Corsi, A., Hallinan, G. W., Lazzati, D., et al. 2018, ApJL, 861, L10
Coulter, D. A., Foley, R. J., Kilpatrick, C. D., et al. 2017, Sci, 358, 1556

Cowperthwaite, P. S., Berger, E., Villar, V. A., et al. 2017, ApJL, 848, L17
Dobie, D., Kaplan, D. L., Murphy, T., et al. 2018, ApJL, 858, L15
Drout, M. R., Piro, A. L., Shappee, B. J., et al. 2017, Sci, 358, 1570
Fong, W., Metzger, B. D., Berger, E., & Özel, F. 2016, ApJ, 831, 141
Ghirlanda, G., Salafia, O. S., Paragi, Z., et al. 2019, Sci, 363, 968
Grandorf, C., McCarty, J., Rajkumar, P., et al. 2021, ApJ, 908, 63
Haggard, D., Nynka, M., Ruan, J. J., et al. 2017, ApJL, 848, L25
Hajela, A., Margutti, R., Alexander, K. D., et al. 2019, ApJL, 886, L17
Hajela, A., Margutti, R., Alexander, K. D., et al. 2021, GCN, 31231, 1
Hajela, A., Margutti, R., Bright, J. S., et al. 2022, ApJL, 927, L17
Hallinan, G., Corsi, A., Mooley, K. P., et al. 2017, Sci, 358, 1579
Hancock, P. J., Murphy, T., Gaensler, B. M., Hopkins, A., & Curran, J. R. 2012, MNRAS, 422, 1812
Horesh, A., Hotokezaka, K., Piran, T., Nakar, E., & Hancock, P. 2016, ApJL, 819, L22
Hotokezaka, K., Kiuchi, K., Shibata, M., Nakar, E., & Piran, T. 2018, ApJ, 867, 95
Hotokezaka, K., & Piran, T. 2015, MNRAS, 450, 1430
Kasen, D., Metzger, B., Barnes, J., Quataert, E., & Ramirez-Ruiz, E. 2017, Natur, 551, 80
Kasliwal, M. M., Nakar, E., Singer, L. P., et al. 2017, Sci, 358, 1559
Kathirgamaraju, A., Giannios, D., & Beniamini, P. 2019, MNRAS, 487, 3914
Kilpatrick, C. D., Foley, R. J., Kasen, D., et al. 2017, Sci, 358, 1583
Klose, S., Nicuesa Guelbenzu, A. M., Michałowski, M. J., et al. 2019, ApJ, 887, 206
Lazzati, D., Perna, R., Morsony, B. J., et al. 2018, PhRvL, 120, 241103
Liu, L.-D., Gao, H., & Zhang, B. 2020, ApJ, 890, 102
Makhathini, S., Mooley, K. P., Brightman, M., et al. 2021, ApJ, 922, 154
Margalit, B., & Piran, T. 2020, MNRAS, 495, 4981
Margutti, R., Alexander, K. D., Xie, X., et al. 2018, ApJL, 856, L18
Margutti, R., Berger, E., Fong, W., et al. 2017, ApJL, 848, L20
McMullin, J. P., Waters, B., Schiebel, D., Young, W., & Golap, K. 2007, in ASP Conf. Ser. 376, Astronomical Data Analysis Software and Systems XVI, ed. R. A. Shaw, F. Hill, & D. J. Bell (San Francisco, CA: ASP), 127
Metzger, B. D. 2017, arXiv:1710.05931
Metzger, B. D., & Bower, G. C. 2014, MNRAS, 437, 1821
Mooley, K. P., Deller, A. T., Gottlieb, O., et al. 2018c, Natur, 561, 355
Mooley, K. P., Frail, D. A., Dobie, D., et al. 2018b, ApJL, 868, L11
Mooley, K. P., Frail, D. A., Ofek, E. O., et al. 2013, ApJ, 768, 165
Mooley, K. P., Nakar, E., Hotokezaka, K., et al. 2018a, Natur, 554, 207
Nakar, E., & Piran, T. 2011, Natur, 478, 82
Nedora, V., Radice, D., Bernuzzi, S., et al. 2021, MNRAS, 506, 5908
O'Connor, B., & Troja, E. 2022, GCN, 32065, 1
Pian, E., D'Avanzo, P., Benetti, S., et al. 2017, Natur, 551, 67
Piran, T., Nakar, E., & Rosswog, S. 2013, MNRAS, 430, 2121
Radice, D., Perego, A., Hotokezaka, K., et al. 2018, ApJ, 869, 130
Ren, J., Lin, D.-B., Zhang, L.-L., et al. 2020, ApJL, 901, L26
Ricci, R., O'Connor, B., & Troja, E. 2022, GCN, 32094, 1
Ricci, R., Troja, E., Bruni, G., et al. 2021, MNRAS, 500, 1708
Shappee, B. J., Simon, J. D., Drout, M. R., et al. 2017, Sci, 358, 1574
Smartt, S. J., Chen, T. W., Jerkstrand, A., et al. 2017, Natur, 551, 75
Tanvir, N. R., Levan, A. J., González-Fernández, C., et al. 2017, ApJL, 848, L27
Troja, E., O'Connor, B., Ryan, G., et al. 2022, MNRAS, 510, 1902
Troja, E., Piro, L., van Eerten, H., et al. 2017, Natur, 551, 71
Valenti, S., Sand, D. J., Yang, S., et al. 2017, ApJL, 848, L24